3-1982

Polynomial Approximations to Mooring Forces in Equations of Low-Frequency Vessel Motions

Bohdan W. Oppenheim
Loyola Marymount University, bohdan.oppenheim@lmu.edu

P. A. Wilson
Southampton University

Journal of Ship Research, Vol. 26, No. 1, March 1982, pp. 16–24

Polynomial Approximations to Mooring Forces in Equations of Low-Frequency Vessel Motions

B. W. Oppenheim[1] and **P. A. Wilson**[2]

Multivariate polynomial approximations are considered to the coupled nonlinear mooring forces acting on a vessel moored with multileg moorings. The objective is to yield explicit forms of equations of the low-frequency vessel motions, since the exact mooring forces are known numerically only. Such forms could then be used for analytical solutions of the equations of motion. It is shown that the polynomials lack sufficient generality and accuracy for this purpose, and hence solution of the problem can be considered only by the exact method.

Introduction

THE OFFSHORE exploration vessels are often kept on station using the so-called multileg mooring systems. Such systems are popular due to their high positioning precision and reliability, as well as their quick deployment and easy maintenance. This type of mooring provides the restoring forces to the vessel by the catenary effects. As the vessel moves under the influence of waves, wind and current, some mooring lines become slacker and some become tauter, thus giving a net restoring force on the vessel.

Typically, a mooring line may contain several segments made of wires, chains and, more recently, synthetic ropes. Wires and chains obey the Hook law and they are relatively heavy. The synthetic ropes are usually nonlinearly elastic and they are light, often even buoyant or neutrally buoyant. Submerged buoys and hung weights are sometimes attached along the lines for improving the catenary performance. Also, surface-floating spring buoys are frequently used in order to improve the spring effect and to facilitate the line deployment. The sea floor is rarely level and its topography affects the line loads and shape considerably. All these effects result in strongly nonlinear mechanics of the mooring lines. A static theory of an arbitrary-composition mooring line is given in [1],[3] where it is shown that, due to the nonlinearities, the solutions can be obtained only numerically. A simplified version of this theory that is utilized in the present calculations is also presented in the Appendix, together with the algorithm used for obtaining the mooring restoring force components acting on the vessel.

The nonlinearities of individual lines also make the total restoring force nonlinear. When this force is resolved into components along and about some vessel axes, the components are also nonlinearly coupled.

The moored vessels experience two distinct types of motions.[4] Small but rapid (high-frequency) motions are induced by individual waves, and large but slow (low-frequency) motions occur due to the second-order slowly varying wave force. The latter force also has a dc component which, together with the wind and current loads, contributes to a steady vessel shift. The high-frequency dynamics have been successfully developed using linear mechanics only, for example, [2, 3]. The low-frequency motions of the vessel in deep waters can be limited to the horizontal plane only, since the vertical motions are orders of magnitude smaller than the horizontal ones and therefore they cause negligible changes of state. The several inherent nonlinearities present in this dynamic problem, besides those of the mooring restoring forces, are as follows. The low-frequency damping is approximately cubic in velocity since it is mostly viscosity-controlled. Since the vessel motions can be large and slow, the effect of the varying weather-incidence angles can contribute large variations of the weather loads, constituting a nonlinear feedback from the vessel yaw motion to the excitation. The large motions also require that two frames of reference be used for defining the equations of motion, one fixed in the vessel for computing the hydrodynamic body forces and one fixed in the earth for computing the mooring restoring forces since the anchors are obviously attached to the earth. The transformations of the motion derivatives and forces between the two frames thus also constitute a source of nonlinearities. The feedback and transformation nonlinearities will vanish, however, if the vessel has a circular symmetry about a vertical axis, for example, disk, sphere and spar.

A solution of the low-frequency nonlinear dynamics has been presented in [4] using time-domain simulation with relative ease. A disadvantage of the simulations, however, is that they can yield only a solution for one particular and complete set of the input conditions at a time, where the inputs include the vessel geometry and mass distribution, mooring system composition, sea bottom topography, and weather conditions. Even a routine mooring design requires many of these inputs to be evaluated and this is both tedious and involved computationally. The simulations of the dynamic parameters in irregular waves must be carried out for many hundreds of cycles in order to yield sufficiently accurate probabilistic and statistical results.

It would thus be desirable to solve the equations in the frequency domain. Such solutions, when available, are convenient in the design since the desired responses of the system can usually be expressed by explicit functions of the terms in the equations of motion, and this form allows for an efficient parametric sensitivity analysis to be performed on individual terms in the functions, or on the input parameters. Also, the frequency-domain solutions would be more efficient computationally, since the entire solution (for all frequencies and all excitation magnitudes) could be obtained in one computer run. For example, judging by the linear version of the moored vessel dynamics, discussed in [4], the computer time of a single simulation, including the statistical processing of the records, is about six times longer than the total computation in the frequency domain.

Unfortunately, no general analytical methods are available for treating the present nonlinear dynamics in their entirety, to the

[1] B. W. Oppenheim, Ph.D. & Associates, Inc., Los Angeles, California.
[2] Ship Science, Southampton University, Southampton, England.
[3] Numbers in brackets designate References at end of paper.
[4] The vessel's flexural vibrations are disregarded in this discussion.
Manuscript received at SNAME headquarters March 31, 1980; revised manuscript received February 17, 1981.

authors' knowledge. Two specific aspects of the problem seem prohibitive, both caused by the large yaw motion allowed, namely, the existance of two frames of reference and the feedback. When the yaw is assumed small (but the remaining motions are allowed to be large), the equations of motion can be formulated in a single equilibrium frame, and the feedback can be neglected. It has been shown in [4] that the small yaw assumption is justified for ships having the mooring line fairleads located sufficiently far from the center of gravity, that is, at bow and stern, and if the motions are not excessive (but they can be larger than the "limits" of the linear motions). Also, in the case of the circular-symmetry vessels, the single frame of reference and the lack of feedback are automatically justified.

With the small yaw assumption the remaining nonlinearities are in the damping and mooring forces. The former are given explicitely by cubics but the latter are available numerically only, thus they have to be expressed by explicit functions in order to proceed with the analytical solutions. This paper addresses the feasibility and practicality of approximating the exact coupled mooring forces by multivariate explicit functions for that purpose. Judging by the literature on the subject of nonlinear vibrations, for example, [5, 6], the solutions seem possible only if the functions are in the form of simple polynomials. The exact forces are computed here using the method given in the Appendix.

A right-handed frame of reference, $Oxyz$, is fixed in the vessel center of gravity in the vessel position where the mean weather loads are in static equilibrium with the mean mooring forces. The x-axis points toward bow and the y-axis to port. The vessel motions along the x- and y-axes are named surge and sway and the rotation about the z-axis, denoted ψ, is named yaw. The exact mooring forces are denoted by three components: $R_x(x,y,\psi)$, $R_y(x,y,\psi)$, and $R_\psi(x,y,\psi)$. The polynomials that approximate them are denoted $P_x(x,y,\psi)$, $P_y(x,y,\psi)$, and $P_\psi(x,y,\psi)$, respectively. In other words, the motions and the forces represent the oscillatory contributions relative to the mean levels. It is important to note that even if the mooring system is initially perfectly symmetric (that is, in the absence of weather elements), the forces defined in the present frame will not be symmetric in general since the static vessel shift to this frame is arbitrary; it depends on the mean weather load.

Constraints imposed on polynomials

The polynomials must be of a fixed composition of terms so that a unique set of the equations of motion can be formulated for all combinations of the mean weather load, mooring stiffness settings, and for any arbitrary assymmetry of the mooring system. A simple mooring design task involves evaluations of a multitude of these combinations. Therefore, if the polynomial composition of terms were allowed to vary, it would mean having to solve just as many different sets of the equations of motion. Typically, the analytical solution of a nonlinear set of equations can be a formidable task in itself. Thus having to solve several such sets would be totally impractical. A unique set of the terms should theoretically be possible since the exact mooring forces are invariant qualitatively. This is a consequence of the fact that the forces vary monotonically, separately in $|x|$, $|y|$, and $|\psi|$, as a result of the mooring lines becoming slacker on the lee side of the vessel and tauter on the weather side, along these vessel motions. Also, the signs of the forces always exhibit the same symmetry/antisymmetry, as shown in Fig. 1.

In order to yield meaningful solutions of the equations of motion, all relevant qualitative behavior of the exact forces should be reflected in the polynomials. Specifically, the coupling, sign symmetries, and the presence of extrema and saddle points should all be represented. Of particular importance is the presence of the actual extrema and the absence of false ones, as this aspect of the behavior influences directly the motion stability problem. A false minimum, for example, would indicate a stable motion center.

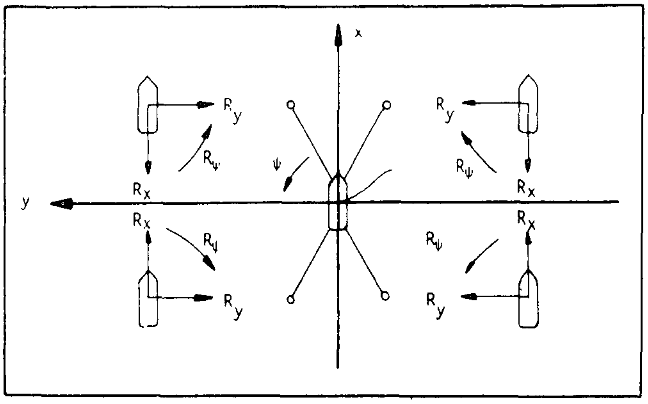

Fig. 1 Signs of mooring forces

Lastly, the approximations should be sufficiently accurate to lead to meaningful and useful results, although no explicit accuracy limit is given here.

Formulation of the polynomials

It is a characteristic feature of multivariate polynomials that by adding some terms to the polynomial composition the approximation may be worsened. [In contrast, in univariate approximation the choice of terms is automatic; terms not needed are assigned (almost) zero coefficients.] Thus in the present case, only those terms should be included which can be justified on physical grounds. It should also be kept in mind that the complexity of the solutions increases sharply with the order and number of the terms. In view of this and in order to avoid false extrema of the approximating functions, the order of the polynomials has been limited to the third, inclusive. A third-order expansion in three variables can be totally controlled in regard to the monotonic behavior. Many of the terms of a higher-order expansion would be quite difficult to be justified from the problem physics.

The present problem has been defined with the assumptions that yaw is small. Therefore the terms containing orders higher than one in yaw motion may be excluded, although this postulation will be verified.

No constant terms are needed in the polynomials because the forces disappear at the origin. This also implies that the error of the approximation will vanish there.

The possible terms under the third-order expansion are therefore as follows: $x,x^2,x^3,y,y^2,y^3,\psi,xy,x^2y,xy^2,x\psi,x^2\psi,y\psi,y^2\psi,xy\psi$. The following subsections examine the terms individually for each force component, P_x, P_y, and P_ψ.

P_x Force component

The force sign is antisymmetric in x, thus odd powers of x are needed. Since the nonlinearity of the force in x may be strong, both x and x^3 are included. The magnitude of the force may not be symmetric, thus the term x^2 is also necessary. The force sign is symmetric in y but the magnitude may not be symmetric, thus the behavior in y alone is described by terms y and y^2. The linear terms are always included, hence also the term ψ. The second-order cross-terms xy, $x\psi$, and $y\psi$ are needed to reflect the asymmetry caused by the arbitrary position of the origin relative to the anchors and the initial asymmetry of the mooring lines. For example, the term xy represents the contribution caused by the diagonal symmetry of the line tensions, as sketched in Fig. 2.

In this case the R_x force will vary more in the $(-x,+y)$ and $(x,-y)$ quadrants and less in the $(+x,+y)$ and $(-x,-y)$ quadrants and this correction is described by the term xy. An analogous situation will exist with the other terms, $x\psi$ and $y\psi$.

Let the third-order cross-terms x^2y, xy^2, $x^2\psi$, and $y^2\psi$ be de-

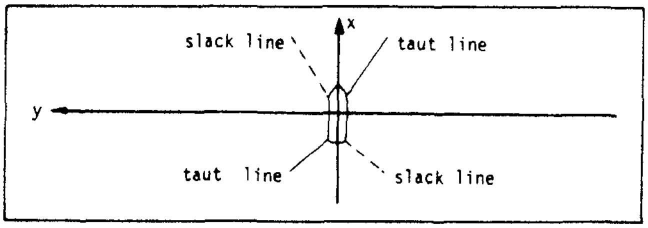

Fig. 2 Basic mooring assymetry

noted m^2n. These terms represent the changes of the force caused by motion along n, due to the system stiffness changes caused by motion in m. To illustrate this point, consider the term xy^2. A motion along y will increase the stiffness in x for both $+|y|$ and $-|y|$, as illustrated in Fig. 3.

Finally, the term $xy\psi$ reflects the changes of the force in one variable due to a simultaneous changes in the two others. The terms which are of order higher than one in ψ have been omitted, in accordance with the small-yaw assumption. Also neglected is the term y^3. The behavior of R_x in y must be nearly quadratic in y and a general lack of symmetry in this direction should be adequately described by the linear term in y. The polynomial thus takes the form (several polynomials will be discussed further and they are denoted by different subscripts, for example, P_{x_1}, P_{y_3}, etc.)

$$P_{x1} = a_{x_1}x + a_{x_2}x^2 + a_{x_3}x^3 + a_{x_4}y + a_{x_5}y^2 + a_{x_6}\psi + a_{x_7}xy + a_{x_8}x^2y + a_{x_9}xy^2 + a_{x_{10}}x\psi + a_{x_{11}}x^2\psi + a_{x_{12}}y\psi + a_{x_{13}}y^2\psi + a_{x_{14}}xy\psi \qquad (1)$$

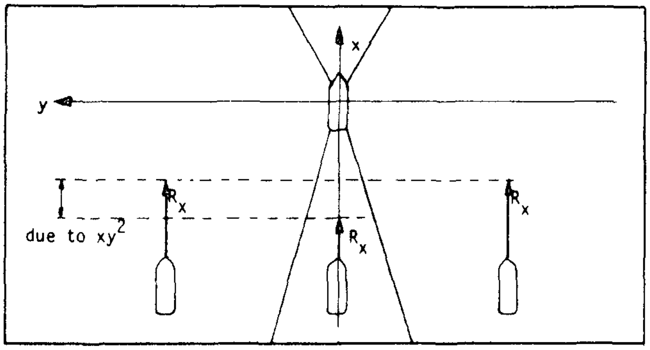

Fig. 3 Surge force contributions due to term xy^2

P_y Force component

This force is analogous to P_x because of the system orthogonality. Specifically, x^3 is dropped and y^3 is included to yield the following form

$$P_{y1} = a_{y_1}x + a_{y_2}x^2 + a_{y_3}y + a_{y_4}y^2 + a_{y_5}y^3 + a_{y_6}\psi + a_{y_7}xy + a_{y_8}x^2y + a_{y_9}xy^2 + a_{y_{10}}x\psi + a_{y_{11}}x^2\psi + a_{y_{12}}y\psi + a_{y_{13}}y^2\psi + a_{y_{14}}xy\psi \qquad (2)$$

P_ψ Force component

The linear terms x, y and ψ are always present. The yaw moment sign is symmetric in the xy space along the diagonal directions; therefore the term xy is needed and it is expected that this component will dominate. There may be nonlinearities in the x- and y-directions separately, and they are described by the linear and quadratic terms in x and y; hence the need for terms x^2 and y^2. The term xy just described results in antisymmetric contributions. The yaw moment may lack symmetry, and thus the variations of xy with x,y and ψ have to be allowed for; hence the terms x^2y, xy^2 and $xy\psi$. Finally, the terms $x\psi$, $x^2\psi$, $y\psi$, and $y^2\psi$ are needed to reflect the system stiffness changes due to the arbitrary rotation of the frame axes relative to the anchors. The terms omitted are the higher orders of ψ and the cubic terms x^3 and y^3. The former are omitted, as before, because of the small-yaw motion, and the latter because the nonlinearity and asymmetry in x and y separately should be adequately represented by x,x^2 and y,y^2 alone. The expression for the moment becomes therefore

$$P_{\psi1} = a_{\psi_1}x + a_{\psi_2}x^2 + a_{\psi_3}y + a_{\psi_4}y^2 + a_{\psi_5}\psi + a_{\psi_6}xy + a_{\psi_7}x^2y + a_{\psi_8}xy^2 + a_{\psi_9}x\psi + a_{\psi_{10}}x^2\psi + a_{\psi_{11}}y\psi + a_{\psi_{12}}y^2\psi + a_{\psi_{13}}xy\psi \qquad (3)$$

Other candidate polynomials

Several other candidates are evaluated in order to verify the preceding selection. One set of these contains all terms possible under expansion up to the third order, including the terms nonlinear in ψ. These are denoted P_{x_2}, P_{y_2} and P_{ψ_2}. They are included to illustrate the validity of the small-yaw assumption:

$$P_{k_2} = a_{k_1}x + a_{k_2}x^2 + a_{k_3}x^3 + a_{k_4}y + a_{k_5}y^2 + a_{k_6}y^3 + a_{k_7}\psi + a_{k_8}\psi^2 + a_{k_9}\psi^3 + a_{k_{10}}xy + a_{k_{11}}x^2y + a_{k_{12}}xy^2 + a_{k_{13}}x\psi + a_{k_{14}}x^2\psi + a_{k_{15}}x\psi^2 + a_{k_{16}}y\psi + a_{k_{17}}y^2\psi + a_{k_{18}}y\psi^2 + a_{k_{19}}xy\psi \quad k = x,y,\psi \qquad (4)$$

The next set of polynomials is similar to the one derived in the foregoing, but with all cross-terms of the third order dropped:

$$P_{x_3} = a_{x_1} + a_{x_2}x^2 + a_{x_3}x^3 + a_{x_4}y + a_{x_5}y^2 + a_{x_6}\psi + a_{x_7}xy + a_{x_8}x\psi + a_{x_9}y\psi$$

Nomenclature

a_{kl} = lth term coefficient in kth polynomial
A_i = cross-sectional area of ith segment
b = unstretched length of mooring line on sea bottom
b^s = stretched length of mooring line on sea bottom
C_i = stretch factor of suspended ith segment
C_i^b = stretch factor of ith segment portion on sea bottom
D = total horizontal span of mooring line
E_i = Young's modulus of ith segment
F_i = proof load of ith segment
H = horizontal tension in mooring line
J = number of mooring lines
L_i = vertical tension at lower end of ith segment
N = number of segments in mooring line
$P(x,y,\psi)$ = polynomial approximating a mooring force component
Q_i = temporary variable
R = vertical reaction at anchor
$R(x,y,\psi)$ = exact mooring force component
s_i = unstretched length of ith segment
s_i^s = stretched length of ith segment
t = touchdown point (where mooring line leaves bottom)
T = axial tension in mooring line
u_i = horizontal span of unstretched ith segment
u_i^s = horizontal span of stretched ith segment
U_i = vertical tension of upper end of ith segment
v_i = vertical span of unstretched ith segment
v_i^s = vertical span of stretched ith segment
w_i = unit wet weight of unstretched ith segment
w_i^s = unit wet weight of stretched ith segment
x,y,ψ = surge, sway, and yaw components

$$P_{y3} = a_{y1}x + a_{y2}x^2 + a_{y3}y + a_{y4}y^2 + a_{y5}y^3 + a_{y6}\psi + a_{y7}xy + a_{y8}x\psi + a_{y9}y\psi$$

$$P_{\psi3} = a_{\psi1}x + a_{\psi2}x^2 + a_{\psi3}y + a_{\psi4}y^2 + a_{\psi5}\psi + a_{\psi6}xy + a_{\psi7}x\psi + a_{\psi8}y\psi \quad (5)$$

The next set is the simplest; it contains only those terms which assure the correct signs of the forces and the basic nonlinearities in the principal directions x and y:

$$P_{x4} = a_{x1}x + a_{x2}x^2 + a_{x3}x^3 + a_{x4}y + a_{x5}y^2 + a_{x6}\psi$$

$$P_{y4} = a_{y1}x + a_{y2}x^2 + a_{y3}y + a_{y4}y^2 + a_{y5}y^3 + a_{y6}\psi \quad (6)$$

$$P_{\psi4} = a_{\psi1}x + a_{\psi2}x^2 + a_{\psi3}y + a_{\psi4}y^2 + a_{\psi5}xy + a_{\psi6}\psi$$

Finally, a polynomial P_ψ is evaluated which contains only the linear terms and a single lowest-order cross-term xy which is necessary for the sign symmetry of the yaw moment:

$$P_{\psi5} = a_{\psi1}x + a_{\psi2}y + a_{\psi3}\psi + a_{\psi4}xy \quad (7)$$

Approximation procedure

The polynomial coefficients are determined by the least-square fit, using the Monte-Carlo method for specifying the data points. In the numerical examples quoted here, 80 equations are formed for up to 19 unknowns, separately for each force component (recall that the maximum number of terms in a polynomial of the third order is 19). Nine of the 80 data points are distributed along the boundaries of the x, y and ψ-space; one point represents zero force at zero motions and the remaining 70 points are distributed in the interior of the x, y, ψ-space using a computer random number generator having a uniform probability distribution.

A typical mooring case is used for the numerical calculations. A Series 60, $C_B = 0.80$ ship displacing 48 117 tonnes (47 155 long tons) is assumed moored with eight identical mooring lines in 333-m-deep (1092 ft) water. The mooring lines have a symmetric spread pattern of 22.5 deg/45 deg. They include a 300-m (984 ft) upper segment of 21.3-kg/m (14.3 lb/ft) wire rope, and a lower chain segment of the weight of 97 kg/m (65 lb/ft). The weather is applied from the direction 15 deg off the bow, thus causing a typical lack of symmetry of the force components upon the shift of the vessel $Oxyz$ origin. The pretension of the lines is made relatively large in order to cause a high stiffness of the system and thus to introduce relatively large nonlinear behavior of the forces. The ship shift from the undisturbed position to the origin turned out to be rather small, above 2 percent of water depth in the x-direction, 0.5 percent in y, and 0.5 deg rotation. These small motions reflect the high mooring stiffness.

The bounds imposed on x, y and ψ within which the approximations are sought and tested are found from practical considerations. The motions of moored platforms used in the oil industry are usually limited to 4 to 8 percent of water depth in the radial direction in the horizontal plane. Motions of about 15 percent depth are often regarded as unsafe, and beyond which there is a danger of entanglement of the lee mooring lines with each other and with underwater obstacles. Thus the range of x and y is taken as

$$|x|_{\max} = |y|_{\max} = 15 \text{ percent water depth}$$

The range of the variable ψ is taken as

$$|\psi| < 1 \text{ deg}$$

This reflects the small-yaw assumption and applies to many of the practical cases.

Criteria for evaluating polynomials

The various polynomials are evaluated using the criteria of the maximum relative error and the total root-mean-square (rms) error of the approximated surface as well as the behavior of that surface in variable ψ. The space of x, y and ψ is defined exactly as that used for fitting the polynomials. The matrix of points at which the errors are computed now contains 30 points in x, 30 in y, and 3 in ψ, all equidistant and all centered about $x = y = \psi = 0$. The errors are defined as follows:

$$e_{\max,k} = \max_{\substack{l=1,2\ldots30\\ m=1,2\ldots30\\ n=1,2,3}} |e_{lmn,k}| \times 100 \text{ percent} \quad (8)$$

$$e_{\text{rms},k} = \left|\frac{1}{2700}\sum_{l=1}^{30}\sum_{m=1}^{30}\sum_{n=1}^{3} e_{lmn,k}^2\right|^{1/2} \times 100 \text{ percent} \quad (9)$$

$$k = x, y, \psi$$

where $e_{lmn,k}$ is the individual relative error

$$e_{lmn,k} = \frac{R_k(x_l,y_m,\psi_n) - P_k(x_l,y_m,\psi_n)}{R_k(x_l,y_m,\psi_n)} \quad (10)$$

The criterion "behavior in ψ" is included in view of the assumed linearity of the forces in ψ. It is a check of whether the approximated forces decrease or increase with ψ where the exact forces do. The results for all polynomials are presented in Table 1. The polynomials P_{k_1}, P_{k_2} and P_{k_3}, $k = x, y, \psi$, are also shown graphically in Figs. 4–6 together with the exact forces, all for the value of ψ of 0 deg. The forces are shown as "floating surfaces" relative to the reference plane corresponding to zero force. Three numbers are listed on the graphs at each corner of the reference plane. They represent the force values corresponding to the value of ψ of −1, 0, and 1 deg, respectively, from top to bottom, for inspecting the behavior of the polynomials in variable ψ. All forces are plotted with the signs reversed, for a better clarity of the graphs. In other words, the graphs show the reactions from the vessel onto the mooring system.

Evaluation of polynomials

It is evident from Table 1 that the polynomials P_{k_2} which contain all terms under the third-order expansion are not the best. This shows that the terms which are of higher orders in ψ are not needed. The polynomials P_{x_1} and P_{y_1}, which were derived from physical considerations, clearly give the best fit. A comparison of these two with P_{x_3} and P_{y_3} confirms that the third-order cross-terms are indeed necessary. A comparison of P_{x_3} and P_{y_3} with P_{x_4} and P_{y_4} gives apparently conflicting results. The presence of the second-order cross-terms has helped P_x but worsened P_y. This is a consequence of the fact that in this particular example the steady vessel shift along y to the frame origin is very small, while along x it is comparatively large. In the reversed situation, however, the necessity of having those terms would then be more evident. The graphs of the P_x and P_y components confirm that the polynomials P_{x_1} and P_{y_1} give a proper qualitative fit. Notice in particular the curvatures of the surfaces along the edges. Also qualitatively good are the all-term polynomials P_{x_2} and P_{y_2}. The polynomials with the third-order cross-terms dropped, P_{x_3} and P_{y_3}, have an improper qualitative behavior, as can be best observed at the edges of the surfaces. Also, the latter two polynomials do not represent properly the behavior in ψ (see the force values in Figs. 4–6). The polynomial forces decrease in ψ where the exact forces increase, and vice versa. In conclusion, the polynomials P_{x_1} and P_{y_1} are the best, as expected from physical considerations of their terms.

The approximations of the yaw moment are much worse than those of the R_x and R_y forces. None of the polynomials has the rms error smaller than 100 percent. This would suggest that the order of the polynomials considered is too low.

As before, the all-term polynomial P_{ψ_2} is inadequate; it is in fact the worst of all those considered. This again is an encouraging

Table 1 Errors of polynomials

Polynomial																				Error, %		Behaviour in ψ
Symbol	Terms Present																			e_{rms}	$\|e_{max}\|$	
P_{x_1}	x	x^2	x^3	y	y^2	-	ψ	-	-	xy	x^2y	xy^2	$x\psi$	$x^2\psi$	-	$y\psi$	$y^2\psi$	-	$xy\psi$	2.0	30.3	OK
P_{x_2}	x	x^2	x^3	y	y^2	y^3	ψ	ψ^2	ψ^3	xy	x^2y	xy^2	$x\psi$	$x^2\psi$	$x\psi^2$	$y\psi$	$y^2\psi$	$y\psi^2$	$xy\psi$	14.9	767.2	OK
P_{x_3}	x	x^2	x^3	y	y^2	-	ψ	-	-	xy	-	-	$x\psi$	-	-	$y\psi$	-	-	-	139.6	6958.0	NO
P_{x_4}	x	x^2	x^3	y	y^2	-	ψ	-	-	-	-	-	-	-	-	-	-	-	-	181.7	9319.0	NO
P_{y_1}	x	x^2	-	y	y^2	y^3	ψ	-	-	xy	x^2y	xy^2	$x\psi$	$x^2\psi$	-	$y\psi$	$y^2\psi$	-	$xy\psi$	0.6	6.3	OK
P_{y_2}	x	x^2	x^3	y	y^2	y^3	ψ	ψ^2	ψ^3	xy	x^2y	xy^2	$x\psi$	$x^2\psi$	$x\psi^2$	$y\psi$	$y^2\psi$	$y\psi^2$	$xy\psi$	0.6	6.4	OK
P_{y_3}	x	x^2	-	y	y^2	y^3	ψ	-	-	xy	-	-	$x\psi$	-	-	$y\psi$	-	-	-	12.1	133.6	NO
P_{y_4}	x	x^2	-	y	y^2	y^3	ψ	-	-	-	-	-	-	-	-	-	-	-	-	6.1	29.1	NO
P_{ψ_1}	x	x^2	-	y	y^2	-	ψ	-	-	xy	x^2y	xy^2	$x\psi$	$x^2\psi$	-	$y\psi$	$y^2\psi$	-	$xy\psi$	258.7	12570.0	OK
P_{ψ_2}	x	x^2	x^3	y	y^2	y^3	ψ	ψ^2	ψ^3	xy	x^2y	xy^2	$x\psi$	$x^2\psi$	$x\psi^2$	$y\psi$	$y^2\psi$	$y\psi^2$	$xy\psi$	467.6	23720.0	OK
P_{ψ_3}	x	x^2	-	y	y^2	-	ψ	-	-	xy	-	-	$x\psi$	-	-	$y\psi$	-	-	-	129.2	6291.0	OK
P_{ψ_4}	x	x^2	-	y	y^2	-	ψ	-	-	xy	-	-	-	-	-	-	-	-	-	113.5	4628.0	OK
P_{ψ_5}	x	-	-	y	-	-	ψ	-	-	xy	-	-	-	-	-	-	-	-	-	181	8579.0	NO

conclusion as it confirms the assumption that no higher powers of ψ are needed. A comparison of the errors between P_{ψ_1}, P_{ψ_3} and P_{ψ_4} suggests that the fit improves when the third- and second-order cross-terms, other than xy, are excluded (xy is necessary for representing the proper symmetries of the yaw moment sign). A comparison of P_{ψ_4} with P_{ψ_5} demonstrates that the nonlinearities and asymmetries of the moment in x and y separately can be strong and therefore the quadratic terms x^2 and y^2 are indeed necessary. Thus the choice must be made between P_{ψ_1}, P_{ψ_3}, and P_{ψ_4}. The plots of the surfaces are rather inconclusive, indicating an adequate qualitative behavior. It should be recalled at this point that the yaw moment of the particular example considered here is rather symmetric because the mooring system is symmetric and also because the steady rotation of the vessel to the frame origin happened to be very small. This obviously gave the apparent result that the cross-terms are not needed. In the general case, however, this may not be so. It is again stressed that for the present purpose it is more important to have a proper qualitative than quantitative approximation. The former would lead to the physically correct (if not very accurate numerically) solutions of equations of motion; therefore a qualitative analysis of the system characteristics could then be performed. On the other hand, a polynomial which happens to give a good quantitative fit in some cases, but does not reflect the physical characteristics of the system, has to be regarded as inadequate. For these reasons the originally derived polynomial P_{ψ_1} is chosen.

Further testing of chosen polynomials

The chosen polynomials P_{k_1} are further tested in five different orientations of the frame origin relative to the anchors. Table 2 presents the motion components from the undisturbed vessel position to the frame origin and the resultant rms and maximum errors of the approximations. The same vessel/mooring system with the same original stiffness is used as before. In other words, the five sets of motions represent five static weather loads of variable strength and direction. Note that all five sets have higher motions than those used in the previous numerical example.

Motion simulation tests

The last test of the polynomials is presented in the form of a comparison between two motion simulations, one with the exact mooring forces and the other with the forces being approximated by the polynomials. Both simulations were performed using the technique and the numerical data of reference [4]. Figures 7 and 8 present the two sets of simulations. The surge and sway motions are shown in percent of water depth, and the yaw is shown in degrees. Table 3 lists the rms values of the motions computed from the random records, as well as the errors of the polynomials for this case. A visual inspection of Figs. 7 and 8 indicates that the approximate motions seem to be identical to the exact ones. This is supported by the numerical values of the motion rms in Table 3. The maximum-motion rms error, that of yaw motion, is only 4.6 percent. This high degree of accuracy occurred because the polynomials happened to be rather well fitted in this particular example, as the values of e_{rms} and e_{max} indicate. The relatively large fitting error of the yaw moment apparently did not greatly affect the motions. This example illustrates that the polynomial approximation can indeed be of high quality in specific cases.

Conclusions

The fixed composition of the terms in the polynomials results in satisfactory accuracy in specific cases and a poor accuracy in some other cases, and it is not possible to predict the error *a priori*. This large variation of the errors is caused by the fact that some of the terms can either improve or worsen the approximation, depending on the specific case. Therefore, in order to achieve a fixed accuracy, the composition of terms would have to vary from one specific case to another.

The order of the polynomials must be kept low in order to assure that the monotonic behavior of the exact forces is reflected in the approximation. This turns out sometimes to be too restrictive in terms of accuracy. Thus again, in order to achieve a desired accuracy, the order of the polynomials would have to be raised, and to assure that the monotonic behavior is preserved the approxi-

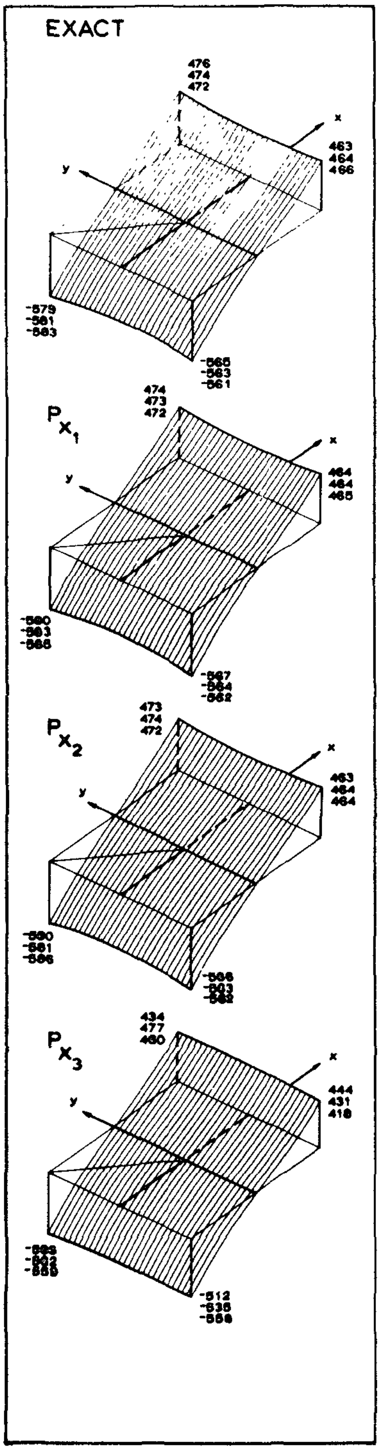

Fig. 4 Exact surge force and polynomials P_{x_1}, P_{x_2}, and P_{x_3}

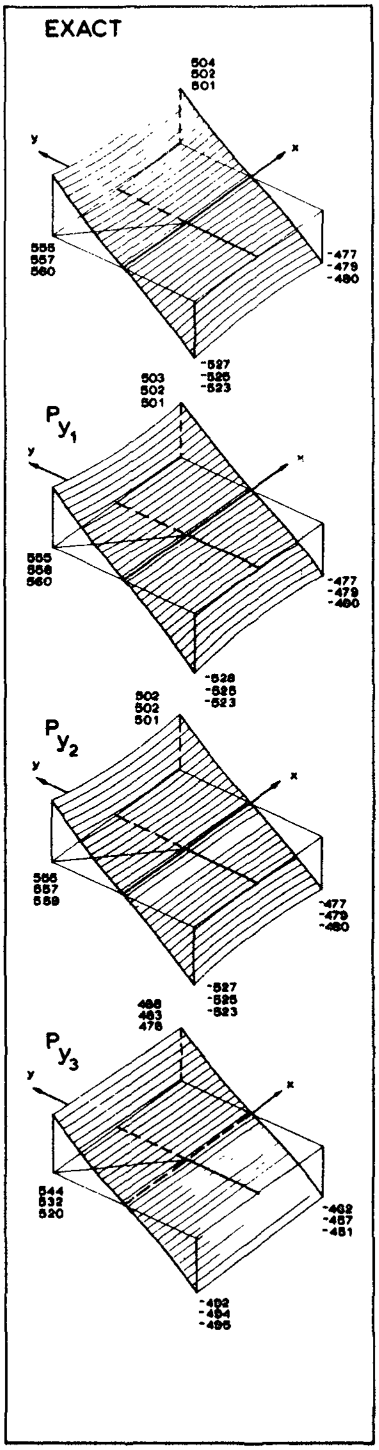

Fig. 5 Exact sway force and polynomials P_{y_1}, P_{y_2}, and P_{y_3}

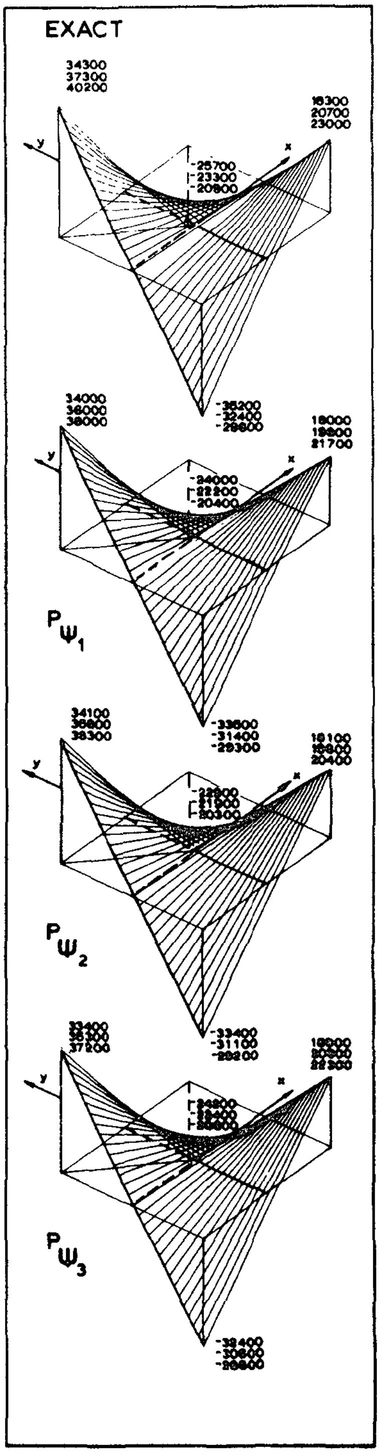

Fig. 6 Exact yaw moment and polynomials P_{ψ_1}, P_{ψ_2}, and P_{ψ_3}

mation would have to be performed by a trial-and-error process individually for each specific case of the exact forces.

The polynomials that have been derived do assure the correct qualitative behavior in the general case. Thus the solution of the equations of motion could in theory be attempted, leading we would hope to a result being correct at least in the qualitative sense. The accuracy of such a solution, however, would vary greatly from case to case. Also, the polynomials are of such a complex form that the analytical solutions would constitute a major task.

It would thus be impractical to proceed with the solutions knowing *a priori* that the accuracy of the results may not be, in general, satisfactory. Whereas in order to achieve a high degree of accuracy it would be necessary to derive the composition of the polynomial terms individually in each specific case, there would be a different set of equations of motion in each case and they would have to be solved individually. This of course would be impractical since the number of weather and stiffness cases that have to be evaluated in a typical mooring design is large.

Motions			Errors, %					
x	y	ψ	p_{x_1}		p_{y_1}		p_{ψ_1}	
% depth	% depth	deg.	e_{rms}	$\lvert e_{max} \rvert$	e_{rms}	$\lvert e_{max} \rvert$	e_{rms}	$\lvert e_{max} \rvert$
-2	0	0	600.	2382.	0.6	70.	211.5	838.
-2	2	0	331.	12940.	245.	5758.	317.	7163.
-2	2	-1	228.	9378.	299.	11670.	1755.	84830.
-2	2	1	654.	30960	170.	7299.	1942.	87890.
0	2	0	0.6	6.2	1452.	6782.	270.	9829.

Table 2 Chosen polynomials in different load conditions

The "behaviour in ψ" is not listed in Table 2 as it is correct in all five cases.

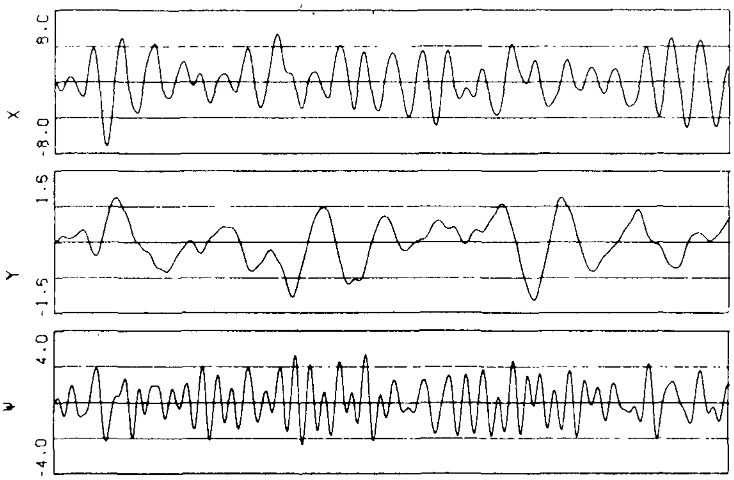

Fig. 7 Simulated motions with exact mooring forces

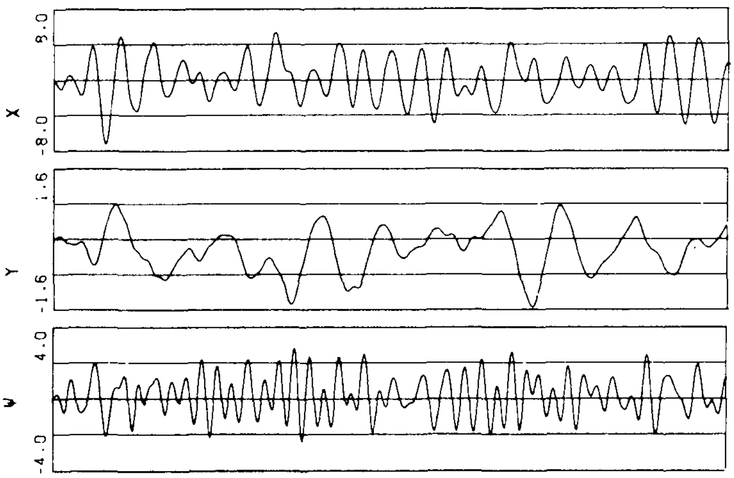

Fig. 8 Simulated motions with mooring forces approximated by polynomials

It is concluded therefore that the only practical way of analyzing the nonlinear dynamics of moorings is to perform the calculations in a time-domain simulation where the mooring forces, given numerically only, can be utilized directly, as demonstrated in [4].

The present calculations were peformed on the ICL2970 computer. The fitting of one polynomial takes about 120 seconds(s) of computer time. One simulation yielding the motion spectral accuracy of about 25 deg of the chi-squared distribution takes about 300 s. The linear solution of the motions in the frequency domain takes 50 s. (The computing time on the CDC7600 machine is approximately 2 to 5 percent of the time on the ICL2970.) It is evident from these time values that the simulations are quite expensive computationally but, in view of the foregoing conclusions, they seem to be the only practical method available.

References

1 Oppenheim, B. W. and Wilson, P. A., "Static 2-D Solution of a Mooring Line of Arbitrary Composition in the Vertical and Horizontal

Table 3 Results of simulations with exact and approximated forces

Item	Component		
	x % water depth	y % water depth	ψ degrees
Exact Motion rms	2.47	0.41	1.08
Approx. Motion rms	2.40	0.40	1.03
Errors of Fitting the Polynomials			
e_{rms} , %	1.1	0.8	180.
$\|e_{max}\|$, %	17.0	5.3	8700.

Operating Modes," *International Shipbuilding Progress* (accepted for publication, 1982).

2 Meyers, W. G., Sheridan, D. J., and Salvesen, N., "Manual NSRDC Ship-Motion and Sea-Load Computer Program," Report No. 3376, David W. Taylor Naval Ship Research and Development Center, Bethesda, Md., 1975.

3 Zarnick, E. E. and Casarela, M. J., "The Dynamics of a Ship Moored by a Cable System Under Sea State," AD-746-490, Report No. 72-5, Catholic University of America, Washington, D.C., 1972.

4 Oppenheim, B. W. and Wilson, P. A., "Low-Frequency Dynamics of Moored Vessels," *Marine Technology*, Vol. 19, No. 1, Jan. 1982, pp. 1-22.

5 Stoker, J. J., *Non-Linear Vibrations*, Interscience, New York, 1950.

6 Wright, J. H. G., "Ship Roll Response and Capsize in Regular and Non-Regular Seas," Report AMTE(H), Ship Science Department, Southampton University, Southampton, England.

Appendix

Calculation of total mooring restoring forces

Let a mooring line consist of N segments ($N > 1$), with the first segment latching onto the anchor. Each segment is described by the following known parameters:

- w_i = unit weight in water of inelastic segment, $w_i > 0$
- s_i = unstretched length
- F_i = proof load
- A_i = cross-sectional area
- E_i = Young's modulus

Figure 9 illustrates the line geometry.

The elementary catenary equations for a segment in an arbitrary loading condition an be shown to be

$$u_i = \frac{H}{w_i} \ln [(U_i + \sqrt{U_i^2 + H^2})/(L_i + \sqrt{U_i^2 + H^2})] \quad (11)$$

$$v_i = \frac{1}{w_i} [\sqrt{U_i^2 + H^2} - \sqrt{L_i^2 + H^2}]$$

where

u_i = horizontal span of suspended ith segment
v_i = vertical span of suspended ith segment
H = horizontal tension in line
U_i = vertical tension in segment at end closer to vessel
L_i = vertical tension in segment at end closer to anchor

Let the touchdown point of the mooring line be denoted by t, not necessarily coinciding with the end of any segment. The un-

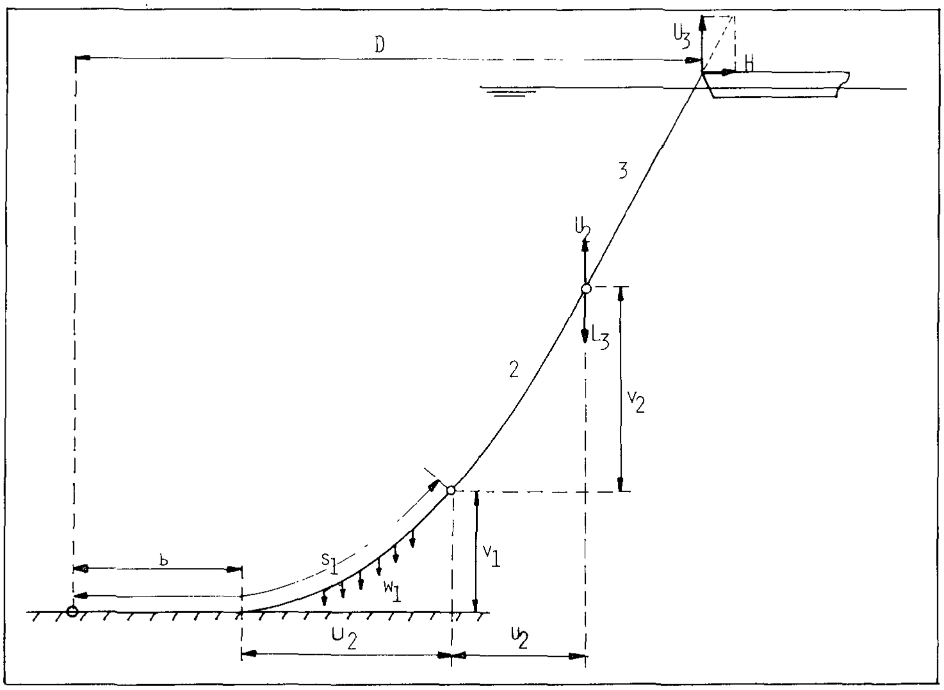

Fig. 9 Geometry of mooring line

stretched length of the line on the sea bottom, b, is then

$$b = \sum_{i=1}^{t} s_i \tag{12}$$

The vertical forces at the segment ends are obtained by summing the line weight from point t upward:

$$L_i = \sum_{j=t}^{i-1} s_j w_j + R \tag{13}$$

$$U_i = L_i + s_i w_i$$

where R is the vertical reaction at the anchor, unknown yet. It should be noted that when $R > 0$, $b = 0$, and when $R = 0$, $b \geqslant 0$. It is assumed that the sea bottom is flat and horizontal. Then any portion of the line on the bottom is entirely supported by the bottom, and the only tension it experiences is H.

Let u_i^s, v_i^s, w_i^s, s_i^s, and b^s denote the stretched values of u_i, v_i, w_i, s_i, and b, respectively. The elongation of the ith segment being in a catenary shape is, from Hook's law

$$\begin{aligned}\Delta s_i &= \frac{1}{A_i E_i} \int_i T(s)\, ds \\ &= \frac{1}{A_i E_i} \int_i \sqrt{(L_i + s w_i)^2 + H^2}\, ds \\ &= \frac{1}{2A_i E_i} \Bigg\{ (L_i + s w_i)\,[H^2 + (L_i + s w_i)^2]^{1/2} + H^2 \ln \\ &\quad \frac{L_i + s w_i + [H^2 + (L_i + s w_i)^2]^{1/2}}{w_i} \Bigg\}_i\end{aligned}$$

Substituting the segment ends for the integral limits

$$L_i + s w_i = \begin{cases} L_i, & s = 0 \\ U_i, & s = s_i \end{cases}$$

the integral takes the form

$$\Delta s_i = \frac{1}{2A_i E_i w_i} \Bigg\{ U_i \sqrt{H^2 + U_i^2} - L_i \sqrt{H^2 + L_i^2} + H^2 \cdot \ln \frac{U_i + \sqrt{H^2 + U_i^2}}{L_i + \sqrt{H^2 + L_i^2}} \Bigg\}$$

Denoting the quantity in the brackets by Q_i, putting $\Delta s_i = s_i^s - s_i$, and rearranging the terms yields the ratio of the stretched length of the segment to the unstretched length, C_i:

$$C_i = \frac{s_i^s}{s_i} = 1 + \frac{Q_i}{A_i E_i w_i s_i} \geqslant 1 \tag{14}$$

For the segment (or a part of it) resting on the bottom, the stretch factor, denoted C_i^b, is available directly from the Hook law:

$$C_i^b = \frac{H s_i}{A_i E_i} \tag{15}$$

The condition of continuity

$$w^s\, ds^s = w\, ds$$

together with equation (14) requires that

$$w_i^s = w_i / C_i$$

Utilizing this result, the spans and length of the stretched segment can be written as products of the unstretched quantities and the stretch factors

$$\begin{aligned} u_i^s &= C_i u_i \\ v_i^s &= C_i v_i \\ s_i^s &= C_i s_i \\ b^s &= \sum_{i=1}^{t} C_i^b s_i \end{aligned} \tag{16}$$

Equations (11)–(16) constitute a set of nonlinear algebraic equations with transcendental functions. They are solved numerically by iterations. The two mutually exclusive domains where solutions are possible are

$$b \geqslant 0, R = 0$$

and

$$b = 0, R > 0$$

The iterations in the first domain first assume a value for b, then H is iterated until the stretched vertical spans of the segments converge to the known vertical distance between the anchor and the vessel fairlead. Similarly in the second domain, R is assumed and H is iterated until the vertical span converges. The independent variable b is varied first, in the range between the value corresponding to the mooring line being almost vertical at the fairlead and zero. Then the independent variable R is varied between zero and the value corresponding to the proof-load of the weakest segment. Next, the results are organized in the order of increasing horizontal span of the entire mooring line. The result of these operations is a systematic series of the mooring line parameters, all given as functions of the line span, D:

$$H(D),\ u_i^s(D),\ v_i^s(D),\ U_i(D),\ L_i(D), \quad i = 1, \ldots, N,\ b^s(D) \text{ and } R(D)$$

The series covers the entire range of the loading conditions of the mooring line. The series is named the Catenary Table and is used in computing the mooring restoring forces acting on the vessel, as described in the following.

The preceding solution is a valid subject with the following limitations:

- The line segments are heavier than water and no buoyant or neutrally buoyant segments are present.
- The bottom is flat and horizontal.
- No submerged buoys or hung weights are attached to the mooring line.
- No surface-floating spring buoys are attached to the line.
- The segments obey the Hook law, thus nonlinearly stretchable synthetic ropes are not allowed.

An extension of the present solution, in which all of the foregoing constraints are eliminated, is given in reference [1] for both the catenary mooring line and the so-called tension-moor line.

Components of mooring restoring forces

The total horizontal mooring restoring force acting on the vessel is the vectorial sum of the horizontal tensions in all the mooring lines. The horizontal tensions are extracted from the Catenary Table by interpolation on the horizontal spans of the individual mooring lines. Let there be J lines in the mooring system. The spans D_j, $j = 1, \ldots, J$, can be found from simple geometry from the vessel position (x,y,ψ), the anchor positions defined in the equilibrium frame (A_{x_j}, A_{y_j}), and from the fairlead coordinates in the body frame (F_{xj}^b, F_{yj}^b), as follows:

$$\begin{aligned} D_j(x,y,\psi) &= [(A_{x_j} - F_{x_j})^2 + (A_{y_j} - F_{y_j})^2]^{1/2} \\ F_{x_j} &= x + F_{xj}^b \cos\psi - F_{yj}^b \sin\psi \\ F_{y_j} &= y + F_{xj}^b \sin\psi + F_{yj}^b \cos\psi, \quad j = 1, \ldots, J \end{aligned}$$

The restoring forces can now be written in the form

$$\left.\begin{matrix} R_x(x,y,\psi) \\ R_y(x,y,\psi) \end{matrix}\right\} = \sum_{j=1}^{J} H_j(D_{j(x,y,\psi)}) \begin{Bmatrix} \cos \\ \sin \end{Bmatrix} \Omega_j$$

$$R_\psi(x,y,\psi) = \sum_{j=1}^{J} H_j(D_{j(x,y,\psi)})\,[F_{xj}^b \cos\Omega_j - F_{yj}^b \sin\Omega_j]$$

where Ω_j is the jth line direction in the body frame of the vessel.